Appl. Phys. B 91, 493–498 (2008)
DOI: 10.1007/s00340-008-3034-2

Applied Physics B
Lasers and Optics

G. LUCAS-LECLIN[1,✉]
D. PABOEUF[1]
P. GEORGES[1]
J. HOLM[2]
P. ANDERSEN[2]
B. SUMPF[3]
G. ERBERT[3]

Wavelength stabilization of extended-cavity tapered lasers with volume Bragg gratings

[1] Laboratoire Charles Fabry de l'Institut d'Optique, CNRS, Univ Paris-Sud, RD128, 91127 Palaiseau, France
[2] Risø National Laboratory, 4000 Roskilde, Denmark
[3] Ferdinand-Braun-Institut für Höchstfrequenztechnik, Albert-Einstein Strasse 11, 12489 Berlin, Germany

Received: 25 September 2007 / Revised version: 25 March 2008
Published online: 15 May 2008 • © Springer-Verlag 2008

ABSTRACT The wavelength stabilization of high-brightness extended-cavity lasers at 810-nm by the use of volume Bragg gratings is described. Narrow linewidth (< 20 pm), high power (2.5 W) and good beam quality ($M^2 < 4$) operation has been obtained in a robust and simple design. The impact of the beam focusing into the Bragg grating on the external cavity performance has been theoretically and experimentally investigated. Finally, second-harmonic generation of the infrared beam has been obtained in a ppKTP crystal, demonstrating a non-linear conversion efficiency of 0.8%/W and up to 8 mW at 405 nm.

PACS 42.40.Pa; 42.55.Px; 42.60.By; 42.65.Ky

1 Introduction

Narrow spectrum, high-brightness semiconductor lasers emitting in the near infrared are of great interest for a wide range of applications, from pumping of rare-earth solid-state lasers to non-linear frequency conversion to the visible for medicine or spectroscopy. The most promising design proposed for high-brightness emission in the 1-W power range is the tapered laser diode [1, 2]. It consists of a single-mode ridge acting as a spatial filter and a large tapered amplifying section. Several achievements have been described in the literature, demonstrating high output powers in a nearly diffraction-limited beam [3–6]. However the large emission spectrum of these devices remains a strong limitation for demanding applications. Monolithic master-oscillator-power amplifier devices, which combine a DBR laser and a power amplifier on the same chip [7], may be utilized but require a complex technology. On the other hand a well-known, efficient way to control the laser spectrum is to use the tapered amplifier as the gain medium in an extended cavity with a spectrally selective component. Usually it consists of a bulk diffraction grating in a Littrow configuration, which allows for both tunability and spectral selectivity [8–10], but fiber Bragg gratings have also been used with the drawback of severe alignment tolerances [11]. Narrow linewidth, high-brightness sources emitting at the Watt level in the near infrared are now commercially available (see for example www.sacher-laser.com or www.toptica.de).

We propose a new and simpler design for the numerous applications in which the emission wavelength is a priori known, and thus large tunability is not desired. The spectrally selective element is a volume reflection grating, which forces the laser emission to the Bragg wavelength, whereas the output power and beam properties are imposed by the tapered amplifier structure. Indeed volume Bragg gratings (VBG) have become essential optical components in the recent years, with a high spectral selectivity, low losses, limited wavelength drift (∼ 0.01 nm/K) and reflectivity from a few % to 100%.[1] Though some experiments have already been reported on the brightness improvement of broad area laser diodes with VBG [12, 13], most of the work has been focused on the wavelength stabilization of single emitters and bars for the pumping of solid-state lasers [14–16]. The Bragg grating has then a low reflectivity, and acts as a perturbative reflective component in a low-feedback external cavity. On the contrary in our set-up the Bragg grating plays the role of a highly reflective mirror of the laser cavity.

In this paper we describe firstly our extended-cavity design for tapered amplifiers using a reflective Bragg grating; the set-up has been validated for lasers around 800 nm. Then we evaluate both theoretically and experimentally the performance of our focused beam configuration, demonstrating a higher mechanical stability without significant decrease of the output power nor spectral selectivity. Finally we report the single-pass frequency-doubling at 405 nm in a periodically poled $KTiOPO_4$ (ppKTP) crystal of the emission of an 810 nm external cavity tapered laser.

2 Description of the external cavity

We have worked with different tapered amplifier structures designed for emission around 800 nm. A super-large optical cavity structure (SLOC) as described in [6] was

✉ Fax: +33-1-64533101, E-mail: gaelle.lucas-leclin@institutoptique.fr

[1] Volume Bragg gratings are provided by PD-LD (www.pd-ld.com), Ondax (www.ondaxinc.com) or Optigrate (www.optigrate.com). Details on their manufacturing processes and glass materials can be found on their respective websites.

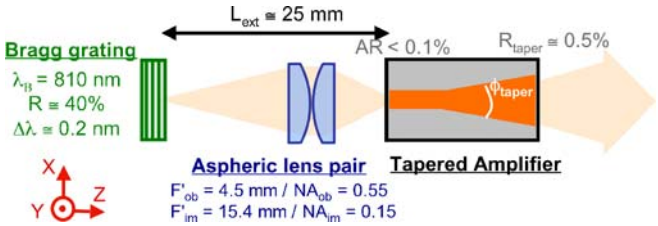

FIGURE 1 Experimental set-up of the external cavity tapered laser with a Bragg grating, in the focused beam configuration

used. The active region consists of a single GaAsP quantum well embedded in a 3-μm thick $Al_{0.45}Ga_{0.55}As$ waveguide. The vertical far-field angle was as low as 18.3° (FWHM) and 95% of the power was included in an angle of 32.5°. The length L_r of the index-guided straight ridge section was between 0.5 to 2 mm, and the angle of the gain-guided tapered section was $\varphi = 4°$. The full amplifier length was 4 mm. The front facet had a reflectivity R_f of 0.5% whereas the rear facet reflectivity R_r was $< 5 \times 10^{-3}$. The devices were mounted p-side (epi-side) down on CuW submounts and, thereafter, on C-mounts. No laser emission was observed from these devices, but amplified spontaneous emission (ASE) in a ~ 25 nm spectral range around 800 nm. With the same design ($L_r = 1$ mm, $\varphi = 4°$) but coatings $R_f \cong 0.1\%$ on the front facet and $R_r \cong 94\%$ on the rear facet, a tapered laser diode has demonstrated an output power of about 4 W and a beam quality parameter $M^2 < 1.9$ [6].

Volume Bragg gratings are realized in photosensitive glasses, which allow writing of periodic structures under UV illumination to make filters with the desired properties [17]. Here we used anti-reflection coated commercial Bragg gratings with a reflectivity in the range 10%–60% and a reflection bandwidth of about 0.2 nm. The Bragg grating acts as a spectrally selective end-mirror of the external cavity, and the useful output power is emitted from the tapered side. The emission from the ridge side of the tapered amplifier is focused into the Bragg grating with a high-NA aspheric lens pair (Thorlabs C230220P: $f'_{coll} = 4.5$ mm 0.55 NA/ $f'_{foc} = 15.4$ mm 0.16 NA) for diffraction-limited imaging (Fig. 1). During the cavity alignment, the lens is fixed to a three-axis (XYZ) translation stage; then it is definitely glued to its optimal position with an epoxy adhesive (Araldite) and the translation stage is removed. No further adjustments of any external cavity components are necessary. The external cavity length is about 25 mm; the whole laser structure is made of copper and is temperature-regulated using a Peltier element.

3 Evaluation of the laser performance

3.1 *Experimental results*

Different tapered amplifiers have been tested in our external cavity set-up (Table 1). With every amplifier the laser emission is strongly locked to the Bragg wavelength whatever the operating current. The spectral linewidth at −3 dB is lower than 20 pm (the measurement being limited by the optical-spectrum analyzer (OSA) resolution) and the side-mode suppression ratio (SMSR) is about 40 dB (Fig. 2). The shift of the emitted wavelength with either the temperature (+6 pm/K) or the operating current remains lower than 0.2 nm, on the entire operating range ($I \leq 4$ A; $T = 15$–45 °C). Actually we have checked that the grating could impose the laser line as long as the Bragg wavelength λ_B is within ±8 nm from the maximum ASE wavelength. Note that thanks to our self-aligned configuration and our monolithic set-up, the external cavity still controls the laser emission on that whole range without re-alignment of the Bragg grating nor the intracavity lens.

Our best results have been obtained with a tapered amplifier with a ridge length of 2 mm and a tapered angle $\varphi = 4°$ (cavity 1). Thanks to the good matching between the grating ($\lambda_B = 798$ nm) and the amplifier gain central wavelength (800 nm at 25 °C), a low threshold current I_{th} of 0.9 A at $T = 25$ °C has been demonstrated, and the output power reached 2.5 W for an operating current of 3.5 A (see Fig. 3). The slope efficiency is typically 1 W/A, and the maximum output power is limited by thermal roll-over and/or facet damages. These results are comparable to those obtained with similar tapered amplifiers but a diffraction grating in a Littrow configuration by Chi and co-authors [9]. It demonstrates that the laser operation is mainly limited by the amplifier itself, not by our experimental set-up. The strong astigmatism of the tapered sources is roughly 500 μm and is easily corrected with one cylindrical singlet lens ($f' = 300$ mm) beyond the collimation aspherical lens ($f' = 8$ mm 0.50 NA). Choosing the adequate focal length allows to circularize the output beam. The design of the amplifier ensured a diffraction-limited emission ($M^2 \leq 1.2$) at low power (≤ 1 W) with a degradation at maximum output power (M^2 equals ~ 3–4). This deterioration of the beam quality with current is attributed on one hand to an insufficient protection against optical feedback on the tapered side in our experimental set-up, and on the other hand to a lower effective reflectivity on the ridge side as compared to tapered lasers with $R_r \cong 94\%$, resulting in an incomplete saturation of the tapered amplifier section [2, 6].

	Volume Bragg grating	Tapered amplifier	Laser thresold maximum output power
Cavity 1	$\lambda_B = 798$ nm, $R_B = 20\%$	$L_r = 2$ mm, $\varphi = 4°$	$I_{th} = 0.9$ A at $T = 25$ °C 2.5 W at 3.5 A
Cavity 2	$\lambda_B = 807.6$ nm, $R_B = 40\%$	$L_r = 0.5$ mm, $\varphi = 4°$	$I_{th} = 2$ A at $T = 17$ °C 1.1 W at 4 A
Cavity 3	$\lambda_B = 809.5$ nm, $R_B = 60\%$	$L_r = 2$ mm, $\varphi = 4°$	$I_{th} = 1.9$ A at $T = 28$ °C $P_{max} = 1.8$ W at $I = 4$ A
Cavity 4	$\lambda_B = 809.5$ nm, $R_B = 60\%$	$L_r = 1$ mm, $\varphi = 4°$	$I_{th} = 1.7$ A at $T = 23$ °C $P_{max} = 1.7$ W at $I = 3$ A

TABLE 1 Description of the four main extended cavities that have been tested. The tapered amplifier chips are described in the text

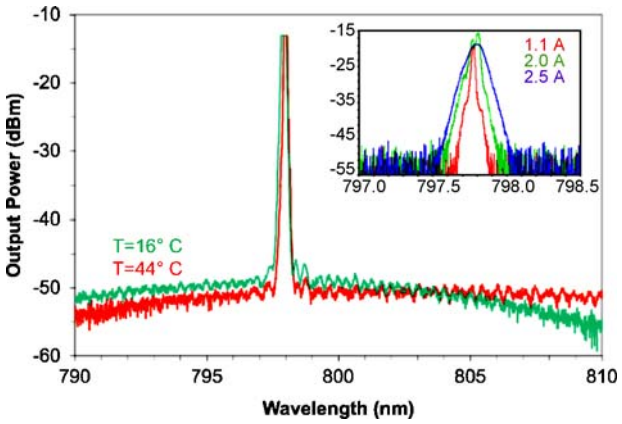

FIGURE 2 Laser spectrum of the tapered source in extended-cavity 1, at different operating temperature and an operating current = 2 A (OSA resolution = 100 pm); the observed SMSR of 35 dB is limited by the saturation of the optical spectrum analyzer. The *inset* shows the enlarged spectrum at various amplifier currents and an operating temperature = 25 °C (OSA resolution = 10 pm)

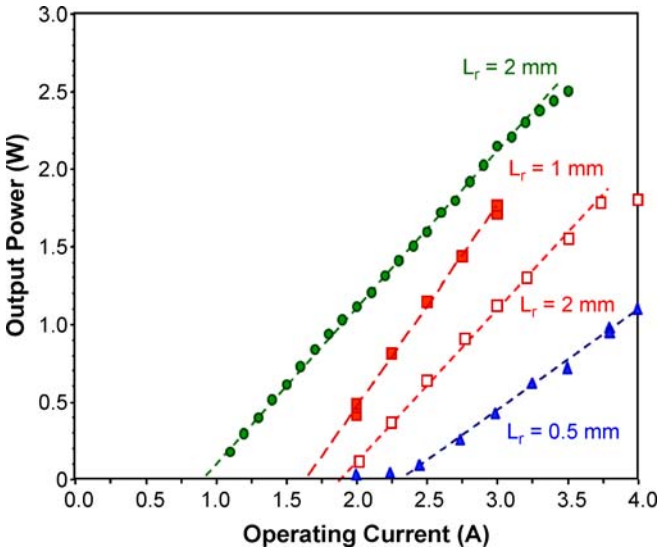

FIGURE 3 Output power as a function of operating current obtained with tapered amplifiers of different geometries ($L_r = 0.5$, 1 and 2 mm, $L_d = 4$ mm, $\varphi = 4°$) and Bragg gratings, respectively, at $\lambda = 809.5$ nm (*red empty* and *filled boxes*), $\lambda = 798$ nm (*green circles*), $\lambda = 807.6$ nm (*blue triangles*)

3.2 *Focused versus collimated configuration*

The main feature of our external cavity set-up is the focusing of the beam inside the Bragg grating, while it has been designed for a collimated beam. The resulting "cat's eye" effect improves the mechanical stability of the laser cavity as in self-aligned Littman cavities [18] or interference filter stabilized external cavities [19, 20]. Here the Bragg grating allows us to take advantage of this helpful effect in both transverse directions with a single component.

The intracavity lens pair has been shifted from its optimal position with the help of a differential three-axis translation stage, the grating and the amplifier being fixed. The resulting output power emitted from the tapered side has been monitored. This has been compared with the misalignments sensitivity of the intracavity lens when the incident beam on the same Bragg grating is collimated with a $f' = 4.5$ mm 0.55 NA aspheric lens (Lightpath 350230). Results are reported in Fig. 4: It is obvious that the focused beam configuration is much less sensitive to transverse misalignments of the lens than the collimated beam one. We evaluate the precision required in X and Y directions to about ± 45 μm for a reduction of the power of 20% with our focused beam configuration. With the collimated beam configuration, the same power decrease is observed for a translation of the lens of only ~ 2 μm. Even in the longitudinal axis is the focused beam configuration slightly less sensitive to misalignments ($\Delta Z = \pm 12$ μm) than the collimated one (± 5 μm). The corresponding angular sensitivity of the grating adjustment is evaluated to ± 10 mrad in the focused beam configuration, and ± 0.3 mrad in the collimated one. Noting that in our operating conditions a 20% power decrease is roughly analogous to a 10% threshold increase, our values are comparable to the ones obtained with other self-aligned set-ups [18, 19].

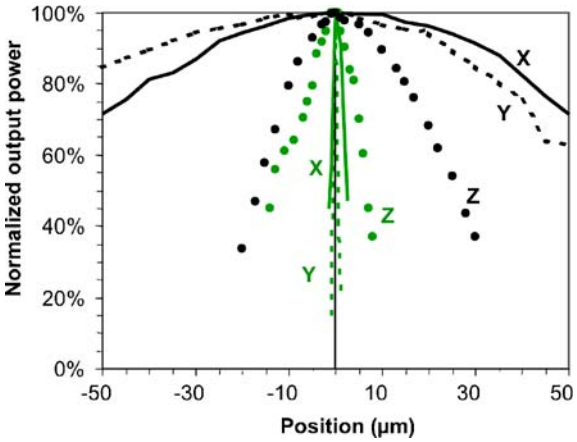

FIGURE 4 Evolution of the output power with intracavity lens pair misalignements in the two transverse directions X (*line*), Y (*dotted line*), and in the longitudinal direction Z (*full circles*) for the focused configuration (*black*) and the collimated beam one (*green*). Measurements made at $I = 1.15 \times I_{th}$

One possible drawback of focusing light inside the grating could be a reduction of its effective reflectivity as well as an increase of its spectral bandwidth. Indeed any deviation of the incident angle from the specified Bragg angle $\theta_B = 0°$ induces a shift of the wavelength reflected by the grating, according to the Bragg relation $\cos(\theta) = \lambda/(2n_0\Lambda)$ for a reflecting volume Bragg grating (VBG) with unslanted index fringes characterized by a thickness d, a grating period Λ, an average index n_0 and an index modulation Δn (see Fig. 5). The diffraction efficiency $\eta(\theta, \lambda)$ is given by [21]:

$$\eta = \left(1 + \frac{1 - \frac{\xi^2}{\nu^2}}{\sinh^2\left(\sqrt{\nu^2 - \xi^2}\right)}\right)^{-1}, \tag{1}$$

with

$$\nu = \pi \frac{\Delta n d}{\lambda \cos\theta}, \quad \text{and} \quad \xi = \pi \frac{d}{\Lambda}\left(1 - \frac{\lambda}{2n_0 \cos\theta}\right).$$

The term ξ characterizes the mismatch to the Bragg condition. The diffraction efficiency within the Bragg conditions

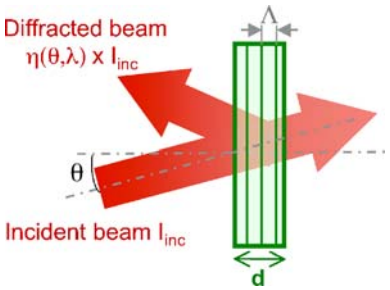

FIGURE 5 Schematic of a reflecting volume Bragg grating

$(\lambda = \lambda_B$ and $\theta = \theta_B)$ is deduced from (1) with $\xi = 0$:

$$\eta_B = \tanh^2\left(\frac{\pi \Delta n d}{\lambda_B \cos\theta_B}\right). \quad (2)$$

Figure 6a presents the variation of η for a typical VBG with respect to wavelength and incident angle. The measured reflectivity of this grating was $\eta_B = 60\%$ at $\lambda_B = 809.5$ nm and normal incidence. The grating thickness d being known, Δn was adjusted to match the experimental η_B value following (2). The theoretical spectral selectivity of that grating is 300 pm (FWHM) at $\theta = 0°$, and its angular selectivity is 60 mrad (3.4°). This latter value is in good accordance with our experimental evaluation of 50 mrad (FWHM) measured under Ti:sapphire illumination (Fig. 6b).

In our extended-cavity set-up, considering the focusing of the beam into the grating, the effective diffraction efficiency of the Bragg grating is given by

$$\eta_\theta(\lambda) = \iint \eta\left(\lambda, \sqrt{\theta_x^2 + \theta_y^2}\right) \times G_{\delta\theta_x \delta\theta_y}\left(\theta_x, \theta_y\right) \mathrm{d}\theta_x \, \mathrm{d}\theta_y, \quad (3)$$

where $G_{\delta\theta_x \delta\theta_y}(\theta_x, \theta_y)$ is the 2D-normalized Gaussian angular distribution of the incident beam with $\delta\theta_x$, and $\delta\theta_y$ the half-widths at $1/e^2$ in the x and y directions:

$$G_{\delta\theta_x, \delta\theta_x}(\theta_x, \theta_y) = \frac{2}{\pi\, \delta\theta_x \delta\theta_x} \exp\left(-\frac{2\theta_x^2}{\delta\theta_x^2}\right) \exp\left(-\frac{2\theta_y^2}{\delta\theta_y^2}\right). \quad (4)$$

The maximum effective diffraction efficiency η_{max} – maximum value of η_θ for given $(\delta\theta_x\ ,\ \delta\theta_y)$ values – has been computed as a function of the divergence angles in Fig. 7. The term η_{max} is typically reduced by a factor of 2 for divergences approximately equal to the angular acceptance of the VBG. In our experimental conditions we roughly estimate $\delta\theta_x = 5° = 0.09$ rad and $\delta\theta_y = 3° = 0.05$ rad from the magnifying ratio of the aspheric lens pair and the beam divergence of the amplifier. The diffraction efficiency of the grating η_{max} is thus decreased to 18%, which remains high enough to control the laser emission. Subsequently, the grating bandwidth is theoretically increased to 0.6 nm. It is worth mentioning here that a higher theoretical efficiency at the Bragg wavelength would have been obtained with a thicker grating but to the detriment of a decreased angular acceptance, leading to an even stronger sensitivity to the focused beam divergence.

In summary, we have demonstrated that the focusing of the light onto the Bragg grating results in a mechanically

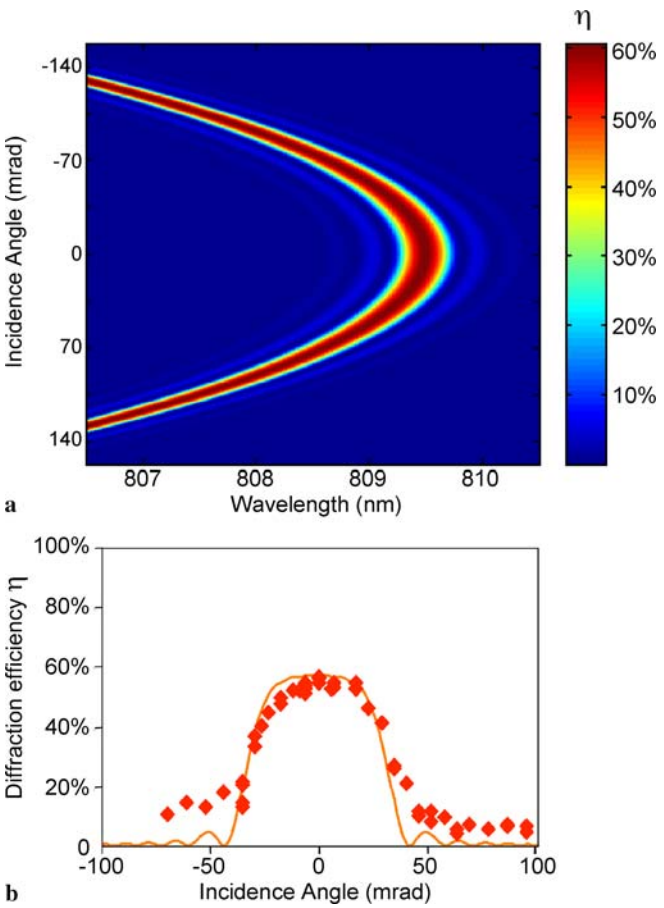

FIGURE 6 (**a**) Diffraction efficiency of a reflective Bragg grating designed at $\lambda_B = 809.5$ nm, with respect to wavelength λ and incidence angle θ ($\lambda_B = 809.5$ nm, $\theta_B = 0°$, $n_0 = 1.50$, $\Delta n = 3.10^{-4}$, $d = 0.7$ mm). (**b**) Experimental (*plot*) and theoretical (*line*) diffraction efficiency of the same Bragg grating as a function of the incidence angle

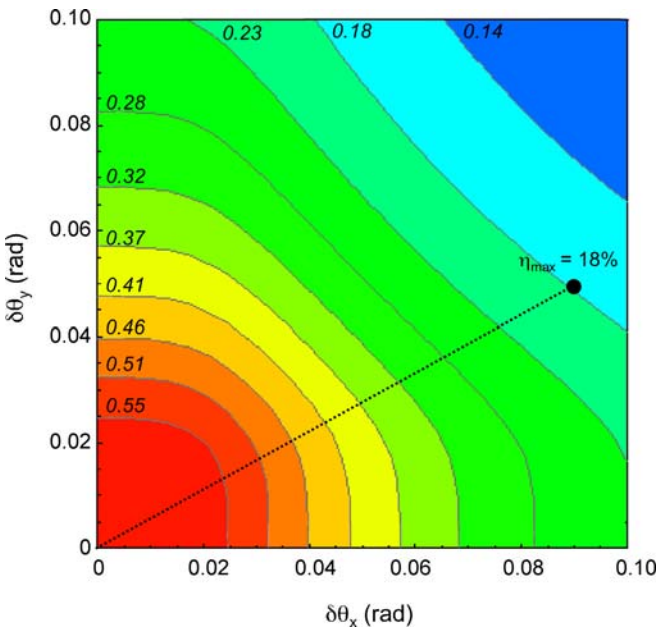

FIGURE 7 Maximum diffraction efficiency η_{max} as a function of the $1/e^2$ half-widths divergence angle $\delta\theta_x$ and $\delta\theta_x$; grating parameters as in Fig. 6

rugged set-up. Moreover we have observed that the external cavity threshold in the collimated beam configuration was 20% higher than in the focused beam configuration, and the achieved output power remains significantly lower at the maximum operating current. We attribute this to the trickier alignment of both the lens and the grating in that cavity. Finally it is noteworthy that here we benefit from the small fast-axis divergence ($\sim 18°$ FWHM) of our tapered amplifiers at 800 nm, which allows us to build a short external cavity with a low magnifying ratio. With amplifiers of larger divergences the external cavity should be longer to maintain the beam focusing angle within acceptable values, without detrimental effects to the cavity mechanical stability.

4 Application to second-harmonic generation in a ppKTP crystal

Finally, the non-linear conversion of the infrared beam inside a ppKTP crystal in a single-pass configuration has been carried out. The non-linear crystal, anti-reflection coated on both facets at 810 and 405 nm, was 10 mm long, and its poling period was 3.4 μm. The temperature of the crystal was set to 49.5 °C, corresponding to the phase-matching temperature at 809.5 nm. The infrared beam from the extended-cavity laser was focused inside the crystal with a 200-mm focal length doublet onto a beam waist diameter of about 43 μm. The entire Rayleigh distance inside the crystal was about 6 mm. The polarization of the fundamental beam was aligned parallel to the non-linear crystal Z axis with a half-wave plate for maximum conversion efficiency.

The maximum emitted power at 405 nm was 8.2 mW for an incident infrared power of 1 W, which results in a non-linear conversion efficiency of 0.8%/W (Fig. 8). This value is as good as the one obtained with the same ppKTP crystal but with a Littrow external cavity tapered laser [9]. It is slightly below the theoretical efficiency evaluated to 1.3%/W with SNLO,[2] taking into account an effective non-linear coefficient $d_{\text{eff}} = 9.8$ pm/V, the focusing of the beam in the middle of the crystal and no internal losses. The M^2 quality parameter of the blue beam has been measured to be $M^2 = 1.0$ in both directions, with a slight astigmatism (≤ 1 mm) stemming from the residual one in the infrared. The second-harmonic generation process was mainly limited by the broadening of the laser line, which becomes comparable to the spectral acceptance bandwidth of the ppKTP (about 50 pm) at high currents. We suspect that this is partly induced by residual feedback from the non-linear crystal into the tapered amplifier resulting in multimode operation of the external cavity laser. This detrimental effect should have been reduced with either a better isolation of the external cavity tapered source from the set-up, an angled incidence on the crystal or a shorter crystal with a larger spectral acceptance.

Though the optical power in the blue remains limited as compared to more complex configurations with external resonant cavities [22], this result demonstrates the capability of our external cavity design for efficient non-linear conversion in the simplest (single-pass) set-up, which requires high brightness and narrow laser line. The non-linear conversion efficiency, and thus the blue power, could even be increased using a waveguide as a non-linear material [23].

[2] SNLO is the free software developed by Sandia National Laboratories (www.sandia.gov), which models non-linear frequency conversion processes in numerous crystals.

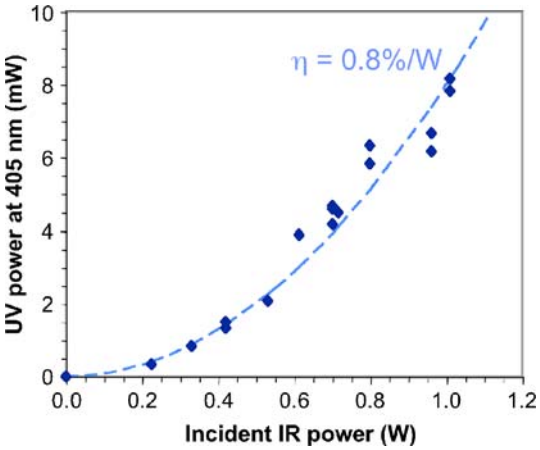

FIGURE 8 Output power at 405 nm vs. the incident infrared power at 810 nm. The *dashed line* shows the quadratic fit of the experimental data

5 Conclusion and outlook

We have demonstrated that a volume Bragg grating may be used as a spectrally selective element to force the emission wavelength of tapered amplifier in an external cavity. We have proposed a compact and robust set-up based on the focusing of the beam inside the grating, which results in a self-aligned configuration with reduced sensitivity to cavity misalignments. The spectral properties of the extended-cavity laser are strongly controlled by the grating, whereas the spatial and power ones result from the amplifier design. Modeling of the grating diffraction efficiency under convergent illumination allowed us to predict the optimized conditions of operation and the effective reflectivity of the grating under experimental conditions. Our set-up has been compared to an external cavity closed by a Bragg grating under collimated illumination from the ridge side, which has resulted in inferior laser performances and more stringent alignment tolerances.

Finally the infrared emission at 809.5 nm from one of our extended-cavity tapered laser has been efficiently converted towards the blue in a ppKTP crystal. The high conversion efficiency that we have obtained illustrates the capability of our set-up for the development of efficient and compact sources in the blue-violet spectral range, which are desired in applications such as biomedical diagnostics. Furthermore our 798-nm laser has been utilized to pump a Nd:ASL crystal, taking advantage from its high brightness and excellent spectral locking; this has provided the very first demonstration of laser emission under diode-pumping at 900 nm from this crystal and its intracavity frequency-doubling with a LBO non-linear crystal [24]. Last but not least, though most of our work has been done around 800 nm, our external cavity design may be applied at any wavelength; indeed we have achieved similar results with different tapered amplifiers emitting at 980 nm and volume Bragg gratings reflecting at this wavelength.

ACKNOWLEDGEMENTS The authors thank the European Community for financial support under the www.BRIGHT.eu program (IP 511722). They are also grateful to P. Sulser (Rainbow Photonics) for his contribution to the SHG experiment. D. Paboeuf acknowledges the funding of his PhD by the French "Délégation Générale de l'Armement".

REFERENCES

1 J.N. Walpole, Opt. Quantum Electron. **28**, 623 (1996)
2 H. Wenzel, B. Sumpf, G. Erbert, CR Physique **4**, 649 (2003)
3 J.N. Walpole, J.P. Donnelly, S.H. Groves, L.J. Missaggia, J.D. Woodhouse, R.J. Bailey, A. Napoleone, IEEE Photon. Technol. Lett. **8**, 1429 (1996)
4 B. Sumpf, R. Hülsewede, G. Erbert, C. Dzionk, J. Fricke, A. Knauer, W. Pittroff, P. Ressel, J. Sebastian, G. Trankle, Electron. Lett. **38**, 183 (2002)
5 M. Kelemen, J. Weber, G. Kaufel, G. Bihlmann, R. Moritz, M. Mikulla, G. Weimann, Electron. Lett. **41**, 1011 (2005)
6 F. Dittmar, B. Sumpf, J. Fricke, G. Erbert, G. Tränkle, IEEE Photon. Technol. Lett. **18**, 601 (2006)
7 H. Wenzel, K. Paschke, O. Brox, F. Bugge, J. Fricke, A. Ginolas, A. Knauer, P. Ressel, G. Erbert, Electron. Lett. **43**, 160 (2007)
8 D. Mehuys, D. Welch, D. Scifres, Electron. Lett. **29**, 1254 (1993)
9 M. Chi, O.B. Jensen, J. Holm, C. Pedersen, P.E. Andersen, G. Erbert, B. Sumpf, P.M. Petersen, Opt. Express **13**, 10 589 (2005)
10 S. Stry, S. Thelen, J. Sacher, D. Halmer, P. Hering, M. Mürtz, Appl. Phys. B **85**, 365 (2006)
11 D. Cornwell, H. Thomas, Appl. Phys. Lett. **70**, 694 (1997)
12 S. Yiou, F. Balembois, P. Georges, J.-P. Huignard, Opt. Lett. **28**, 242 (2003)
13 G. Venus, V. Rotar, L. Glebov. Paper presented at the 26th Annual Conference on Lasers and Electro-Optics. CLEO/IQES and PhAST Technical Digest, Long Beach, CA, May 2006, paper CFG4
14 B. Volodin, S. Dolgy, E. Melnik, E. Downs, J. Shaw, V. Ban, Opt. Lett. **29**, 1891 (2004)
15 G. Venus, A. Sevian, V. Smirnov, L. Glebov, Proc. SPIE **5711**, 166 (2005)
16 Y. Zheng, H. Kan, Opt. Lett. **30**, 2424 (2005)
17 O. Efimov, L. Glebov, K. Richardson, V. Smirnov, Appl. Opt. **38**, 619 (1999)
18 B. Fermigier, G. Lucas-Leclin, J. Dupont, F. Plumelle, M. Houssin, Opt. Commun. **153**, 73 (1998)
19 P. Zorabedian, W. Trutna, Opt. Lett. **13**, 826 (1988)
20 X. Baillard, A. Gauguet, S. Bize, P. Lemonde, Ph. Laurent, A. Clairon, P. Rosenbusch, Opt. Commun. **266**, 609 (2006)
21 H. Kogelnik, Bell. Syst. Tech. J. **48**, 2909 (1969)
22 J. Bhawalkar, Y. Mao, A. Goyal, P. Gavrilovic, Y. Conturie, S. Singh, Opt. Lett. **24**, 823 (1999)
23 T. Sugita, K. Mizuuchi, Y. Kitaoka, K. Yamamoto, Opt. Lett. **24**, 1590 (1999)
24 D. Paboeuf, G. Lucas-Leclin, P. Georges, B. Sumpf, G. Erbert, C. Varona, P. Loiseau, G. Aka, B. Ferrand, In: *Advanced Solid-State Photonics*, OSA Technical Digest Series (CD) (Optical Society of America, 2007), paper WB20